PLANT SCIENCE TODAY
Vol x(x): xx–xx
https://doi.org/10.14719/pst.10092

eISSN 2348-1900

RESEARCH ARTICLE

# Screening and selection of a lead phytochemical inhibitor against Nsp3 protein, from *Lawsonia inermis* L. through *in silico* approaches

**Debapriya Das[1], Sujata Dhar Dutta[2], Bidisha Mallick[1], Dipu Samanta[3] & Debleena Roy[1*]**

[1]Post Graduate Department of Botany, Lady Brabourne College, P-1/2 Suhrawardy Avenue, Beniapukur, Kolkata 700 017, West Bengal, India
[2]Department of Zoology, Lady Brabourne College, P-1/2 Suhrawardy Avenue, Beniapukur, Kolkata 700 017, West Bengal, India
[3]Department of Botany, Dr. Kanailal Bhattacharyya College, Howrah 711 104, West Bengal, India

*Correspondence email - debleena.roy@ladybrabourne.com

Received: 16 June 2025; Accepted: 11 September 2025; Available online: Version 1.0: 23 December 2025

**Cite this article:** Debapriya D, Sujata DD, Bidisha M, Dipu S, Debleena R. Screening and selection of a lead phytochemical inhibitor against Nsp3 protein, from *Lawsonia inermis* L. through *in silico* approaches. Plant Science Today (Early Access). https://doi.org/10.14719/pst.10092

## Abstract

*Lawsonia inermis* L., a plant of immense significance as the natural source of dye "*Mehendi*" is rich in secondary metabolites that impart important medicinal properties. These phytochemicals offer plant-based alternatives to synthetic drugs, which are often associated with harmful side effects, reinforcing the need to explore such natural compounds. The main objective of this study is to find plant-based lead from among the phytochemicals present in *Lawsonia inermis* L., against Nsp3 protein. Methanolic extracts from the plant was used and a group of phytochemicals were verified and identified by ultra-high-performance liquid chromatography coupled with quadrupole time-of-flight mass spectrometry, which were then subjected to phytochemical screening. The shortlisted best ligands (caffeic acid and lawsone) were subjected to molecular dynamic simulations for 100 ns, where RMSD, Rg and RMSF were analysed along with the binding affinities to the protein. Lawsone and caffeic acid emerged as good candidates. Molecular dynamic simulations indicated that lawsone, a naphthoquinone, formed stable complexes with Nsp3, exhibiting favourable RMSD, RMSF and Rg values, as well as a strong binding affinity of -20.72 kcal/mol. Our analysis shows the prospective possibility of lawsone, as a potential antiviral compound. This also highlights the interactions of a naphthoquinone, against Nsp3 protein, increasing the medicinal importance of the plant. Previous studies usually reveal phenols and flavonoids to be effective antiviral agents. This study, for the very first time, reveals the potential of lawsone (naphthoquinone and the main pigment of the plant), against Nsp3 protein.

**Keywords:** docking; *Lawsonia inermis*; molecular dynamics; Nsp3; phytochemicals; screening

## Introduction

India with its rich diversity of medicinal plants stands tall among the countries which have a long history of plant-based medicines (1-4). Ayurveda which originated around 5000 years ago is gradually witnessing an era of commercialization, with a rise in demand for alternatives to diseases, with less harmful side-effects (5,6). The market of medicinal plants in India, is expected to value at around 8 billion US dollars by 2022. A knowledge and practise which originated in India, is slowly spreading globally, providing potential cure and treatment to many (7). Dravyaguna, a part of Ayurveda dealing with the properties and uses of medicinal plants, has mention of Madyantika, or *Lawsonia inermis*, being useful in the commercial and medicinal sectors (8). Some of the important medicinal properties of *Lawsonia inermis*, include, anti-carcinogenic, immune-stimulatory, antidiabetic, antiproliferative and many more (9-11). This can be attributed to the bioactive compounds present in the plant, especially which are rich in phenols and flavonoids (12,13).

Herbal medicines use a strong combination of bioactive compounds, which have less toxic side effects, providing therapeutic benefits with reduced toxicity (14,15). Although, vaccines serve to be effective, there have been reports of many side effects and they are comparatively costly (16,17). Natural bioactive compounds (phenols and flavonoids) serve as effective antiviral agents by hindering viral replication, translation, transcription, viral packaging and assembly (18,19). Quercetin, apigenin, naringenin, curcumin, chebulagic acid and punicalagin have shown effective action against viruses like HIV, DENV, Influenza and others (20,21). The antiproliferative potential of polyphenols is of utmost importance, as they have been reported to inhibit a wide range of viruses like, influenza virus, coronavirus, rhinovirus, syncytial virus, rotavirus, hepatitis virus, herpes virus, dengue virus and many more (22,23). Hence, in this study, we aim to find plant-based alternatives, from *Lawsonia inermis* L., whose mention has been found in the Ayurvedic texts (9,24). The phytochemicals identified were analysed against Nsp3, an important protein needed for the maintenance of the viral life cycle of SARS-CoV-2 (25).

Among the many important roles played by Nsp3 protein, it aids in polyprotein processing by binding to viral proteins (26). Nsp3 protein, along with Nsp4 and Nsp6 are involved in formation of Double-Membrane Vesicles (DMV) in coronavirus-infected cells, playing a key role in virus survival (27,28). Apart from this, the protein also helps in virus replication, by interacting with 3CLpro and PLpro (27,29). Methanolic extracts of *Lawsonia inermis* L., were seen as potential sanitizers, exhibiting strong antimicrobial activity, suggesting their role in bacterial and viral growth inhibition (30). The target protein Nsp3 holds immense importance in the virus survival. Hence, targeting this protein can substantially lower the pathogenicity of the virus, providing a plant-based alternative (31). Based on previous analyses, this work, for the very first time investigates the interaction of identified bioactive compounds from *Lawsonia inermis* L., against the Nsp3 protein.

## Materials and Methods

### Preparation of protein

Nsp3, the largest multidomain protein encoded by the virus has an average molecular weight of 200kDa (32). The structure was obtained from RCS PDB database (Fig. 1). For processing the PDB protein file, MGL tools were used, where, polar hydrogens were added, ligand and water molecules were removed before docking.

### Ligand preparation

Seeds of *Lawsonia inermis* L. were obtained from the National Bureau of Plant Genetic Resources (NBPGR), New Delhi (IC 627437). Leaves of four-month-old *Lawsonia inermis* L. were dried, weighed, crushed and kept in 80 % methanol overnight for optimum extraction of phytochemicals (33). The leaf extract was subjected to Ultra-High-Performance Liquid Chromatography Quadrupole Time-of-Flight Mass Spectrometry (UHPLC–QTOF-MS) (Agilent UHPLC–QTOF-MS model 6500 series). For the process, 10 µL sample was injected, using Acquity UPLC BEH C18 column (100 mm x 2.1 mm, 1.7 µm) (34), with gradient mobile phases, A: ultrapure water (0.5 % acetic acid) and B: acetonitrile: methanol (50:50). A group of 14 phytochemicals (Fig. 2) were reported among which some were validated from the list provided in a previous work (35), along with which, some more compounds were also identified. Table 1 summarises the data from the PubChem Database.

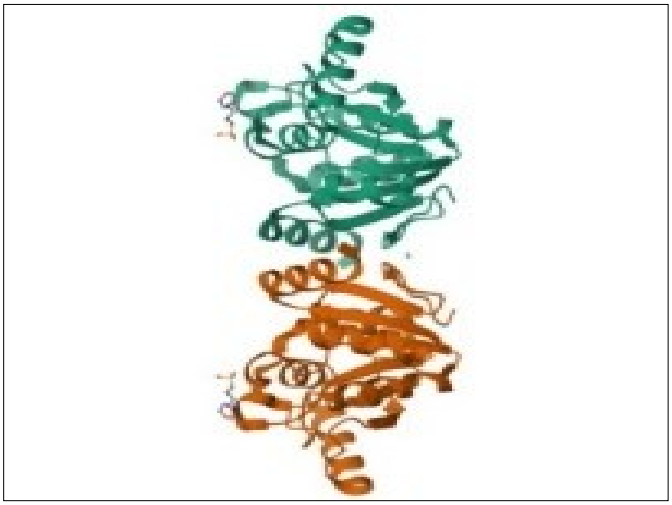

**Fig. 1**. Protein Nsp3 (PDB ID: 8AZC) downloaded from the RCSB PDB.

### Docking analysis of ligand with the protein

Docking was done by AutoDock Vina (15), against the Nsp3 protein. Following which, the complexes were further processed for molecular dynamic simulations for 100 ns, with the CHARMM ffT92 force field (15). The log file obtained gave 9 poses for the ligand-protein complexes, along with RMSD values and binding affinity. Poses with the highest binding affinity and low RMSD values (less than 2Å) were considered (36). The interactions were recorded using the Discovery Studio (https://www.3ds.com/products/biovia/discovery-studio) and the interacting residues were noted, along with the number of hydrogen bonds.

### Lipinski's rule of five

Ligands were analysed using Lipinski's rule of five, which highlights the drug "potential" of a ligand (http://www.scfbio-iitd.res.in/software/drugdesign/lipinski.jsp) (37).

### *In silico* ADME analysis

Swiss ADME was used to study the behaviour of the ligands in the human body by, analysing characteristics such as metabolism, absorption, excretion and distribution (http://www.swissadme.ch/index.php) (38,39).

### Bioactivity score

This parameter helps us to know about the interaction of the prospective drug candidates with the drug receptors present in the body, done by Molinspiration software (https://www.molinspiration.com/). A bioactivity score of 0 and more, shows good bioactivity, whereas lower scores indicate poor activity (40,41).

### ADMET analysis

This analysis can help predict the performance of a drug in the body (42,43), which is done by ADMET analysis.

### Molecular dynamic simulations

AutoDock Vina and Discovery Studio give a very stringent overview of the proteins-ligand interactions (44). This limitation can be overcome by molecular dynamic simulations between complexes, in a solvation box, for a specific time-period (45,46). From the previous analysis, lawsone and caffeic acids were shortlisted which were further analysed (47). GROMACS is a versatile program and can be easily customized. For charge neutralization, 2 sodium atoms were added to each of the systems, which further aided in the smooth running of the simulations (48).

The force field used in the dynamic studies were CHARMM36 (charmm36-jul2022) and the SPC water model. The energy minimization was done, which ensures structural stability. Once the system was energy minimized and evaluated as positive for potential energy (Fig. 3), we achieved equilibration for the same. The equilibration was done for temperature and pressure both (The system was equilibrated within 1 ns). This was achieved at temperature equilibration in 1000 ps [1 ns, maintaining an average temperature of 300.022 K]. Temperature equilibration was done to increase system stability before simulation (49). In addition, the system got pressure equilibrated within 1000 ps, maintaining an average pressure of -0.258134 bar. The above process of energy minimization and equilibration (temperature & pressure) ensures structural stability, needed for further processing of molecular dynamic simulation by GROMACS. The system was simulated for 100 ns and the trajectory was recorded every 10 ps.

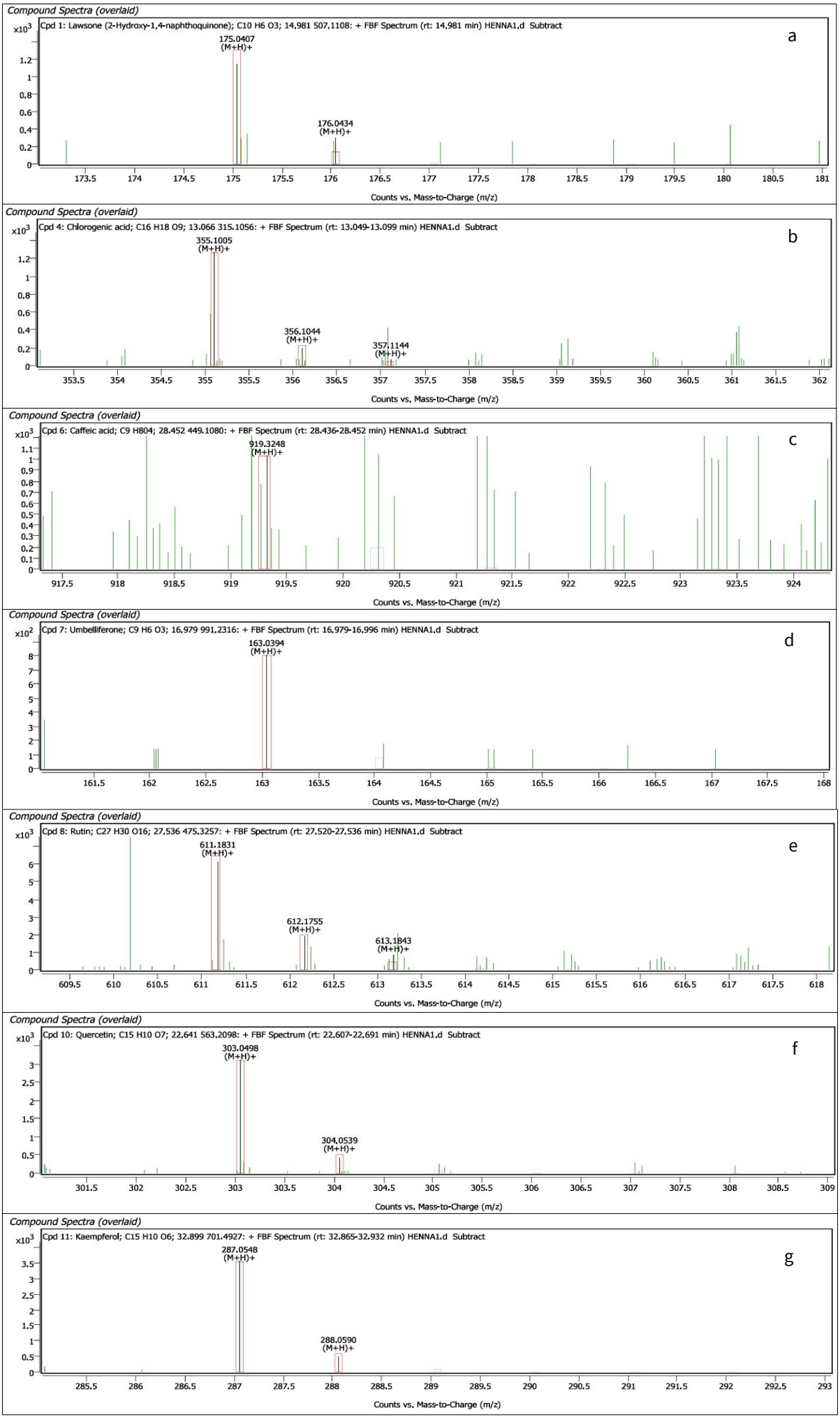
Compound Spectra (overlaid)
Cpd 1: Lawsone (2-Hydroxy-1,4-naphthoquinone); C10 H6 O3; 14.981 507.1108: + FBF Spectrum (rt: 14.981 min) HENNA1.d Subtract
175.0407 (M+H)+
176.0434 (M+H)+
a
Counts vs. Mass-to-Charge (m/z)
Compound Spectra (overlaid)
Cpd 4: Chlorogenic acid; C16 H18 O9; 13.066 315.1056: + FBF Spectrum (rt: 13.049-13.099 min) HENNA1.d Subtract
355.1005 (M+H)+
356.1044 (M+H)+
357.1144 (M+H)+
b
Counts vs. Mass-to-Charge (m/z)
Compound Spectra (overlaid)
Cpd 6: Caffeic acid; C9 H804; 28.452 449.1080: + FBF Spectrum (rt: 28.436-28.452 min) HENNA1.d Subtract
919.3248 (M+H)+
c
Counts vs. Mass-to-Charge (m/z)
Compound Spectra (overlaid)
Cpd 7: Umbelliferone; C9 H6 O3; 16.979 991.2316: + FBF Spectrum (rt: 16.979-16.996 min) HENNA1.d Subtract
163.0394 (M+H)+
d
Counts vs. Mass-to-Charge (m/z)
Compound Spectra (overlaid)
Cpd 8: Rutin; C27 H30 O16; 27.536 475.3257: + FBF Spectrum (rt: 27.520-27.536 min) HENNA1.d Subtract
611.1831 (M+H)+
612.1755 (M+H)+
613.1843 (M+H)+
e
Counts vs. Mass-to-Charge (m/z)
Compound Spectra (overlaid)
Cpd 10: Quercetin; C15 H10 O7; 22.641 563.2098: + FBF Spectrum (rt: 22.607-22.691 min) HENNA1.d Subtract
303.0498 (M+H)+
304.0539 (M+H)+
f
Counts vs. Mass-to-Charge (m/z)
Compound Spectra (overlaid)
Cpd 11: Kaempferol; C15 H10 O6; 32.899 701.4927: + FBF Spectrum (rt: 32.865-32.932 min) HENNA1.d Subtract
287.0548 (M+H)+
288.0590 (M+H)+
g
Counts vs. Mass-to-Charge (m/z)

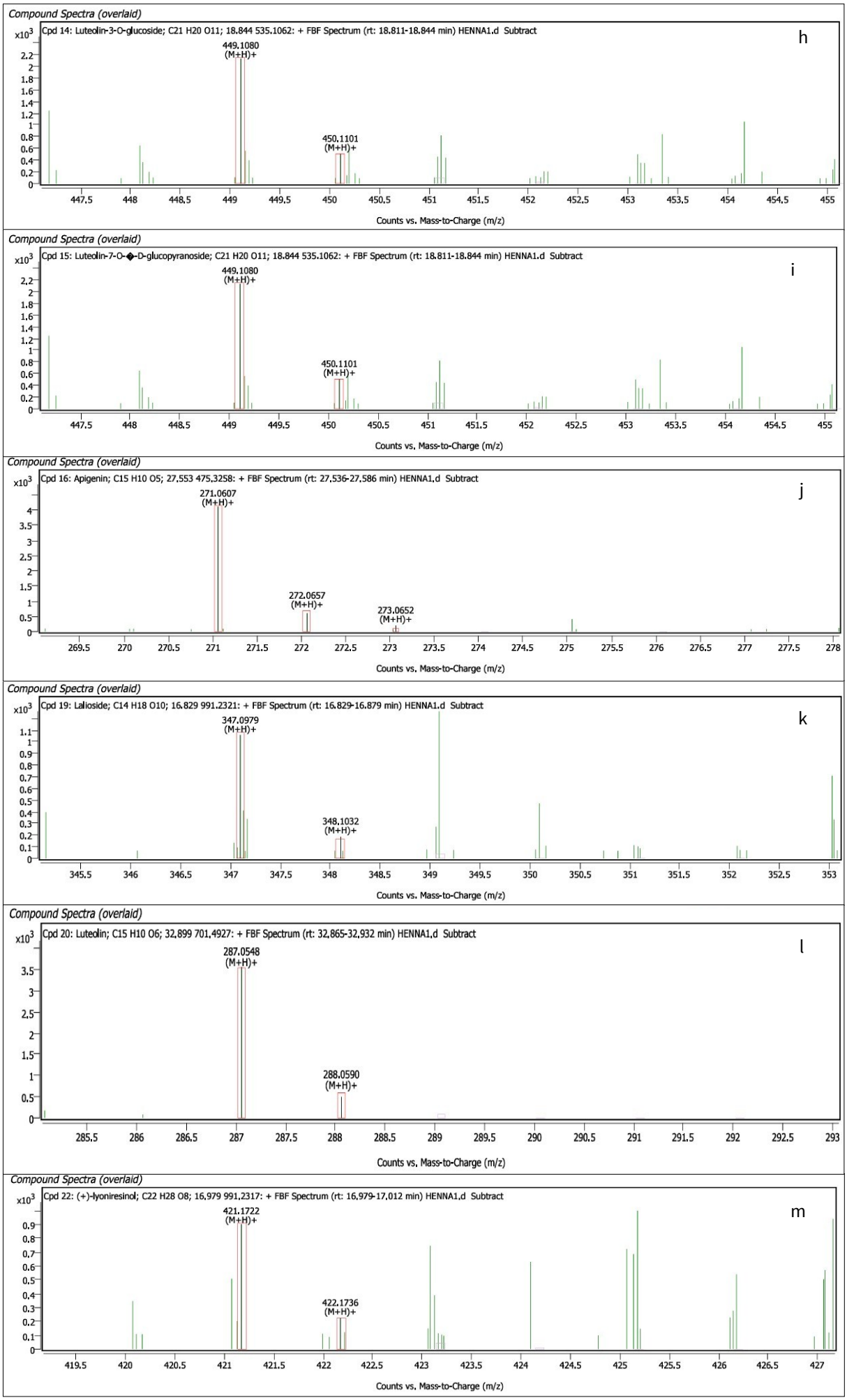
Compound Spectra (overlaid)
Cpd 14: Luteolin-3-O-glucoside; C21 H20 O11; 18.844 535.1062: + FBF Spectrum (rt: 18.811-18.844 min) HENNA1.d Subtract
449.1080 (M+H)+
450.1101 (M+H)+
h
Counts vs. Mass-to-Charge (m/z)
Compound Spectra (overlaid)
Cpd 15: Luteolin-7-O-◆-D-glucopyranoside; C21 H20 O11; 18.844 535.1062: + FBF Spectrum (rt: 18.811-18.844 min) HENNA1.d Subtract
449.1080 (M+H)+
450.1101 (M+H)+
i
Counts vs. Mass-to-Charge (m/z)
Compound Spectra (overlaid)
Cpd 16: Apigenin; C15 H10 O5; 27.553 475.3258: + FBF Spectrum (rt: 27.536-27.586 min) HENNA1.d Subtract
271.0607 (M+H)+
272.0657 (M+H)+
273.0652 (M+H)+
j
Counts vs. Mass-to-Charge (m/z)
Compound Spectra (overlaid)
Cpd 19: Lalioside; C14 H18 O10; 16.829 991.2321: + FBF Spectrum (rt: 16.829-16.879 min) HENNA1.d Subtract
347.0979 (M+H)+
348.1032 (M+H)+
k
Counts vs. Mass-to-Charge (m/z)
Compound Spectra (overlaid)
Cpd 20: Luteolin; C15 H10 O6; 32.899 701.4927: + FBF Spectrum (rt: 32.865-32.932 min) HENNA1.d Subtract
287.0548 (M+H)+
288.0590 (M+H)+
l
Counts vs. Mass-to-Charge (m/z)
Compound Spectra (overlaid)
Cpd 22: (+)-lyoniresinol; C22 H28 O8; 16.979 991.2317: + FBF Spectrum (rt: 16.979-17.012 min) HENNA1.d Subtract
421.1722 (M+H)+
422.1736 (M+H)+
m
Counts vs. Mass-to-Charge (m/z)

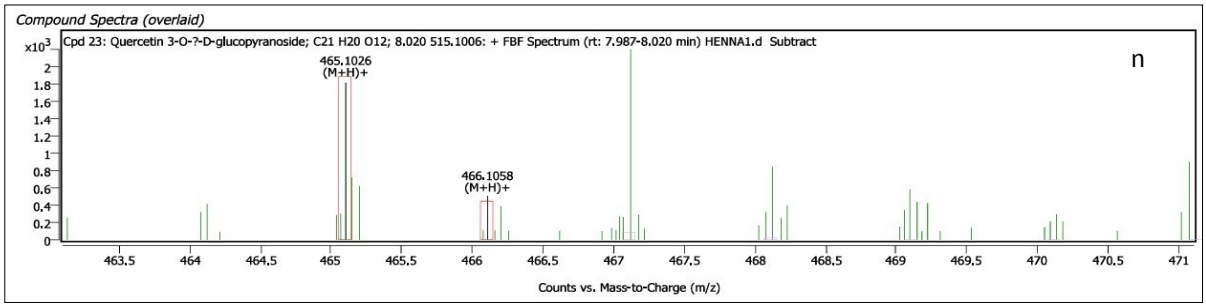


**Fig. 2.** MS spectrum of phytochemicals.

a) Lawsone; b) Chlorogenic acid; c) Caffeic acid; d) Umbelliferone; e) Rutin; f) Quercetin; g) Kaempferol; h) Luteolin-3-O-glucoside; i) Luteolin-7-O-β-D-glucopyranoside; j) Apigenin; k) Lalioside; l) Luteolin; m) Lyoniresinol; n) Quercetin-3-O-β-D-glucopyranoside

**Table 1**. Identified phytochemicals with their PubChem ID and formula

| Sl. No | Name | PubChem ID | Chemical formula |
|---|---|---|---|
| 1 | Lawsone | 6755 | $C_{10}H_6O_3$ |
| 2 | Chlorogenic acid | 1794427 | $C_{16}H_{18}O_9$ |
| 3 | Caffeic acid | 689043 | $C_9H_8O_4$ |
| 4 | Umbelliferone | 5281426 | $C_9H_6O_3$ |
| 5 | Rutin | 5280805 | $C_{27}H_{30}O_{16}$ |
| 6 | Quercetin | 5280343 | $C_{15}H_{10}O_7$ |
| 7 | Kaempferol | 5280863 | $C_{15}H_{10}O_6$ |
| 8 | Luteolin-3-O-glucoside | 12309350 | $C_{21}H_{20}O_{11}$ |
| 9 | Luteolin-7-O-β-D-glucopyranoside | 5280637 | $C_{21}H_{20}O_{11}$ |
| 10 | Apigenin | 5280443 | $C_{15}H_{10}O_5$ |
| 11 | Lalioside | 189452 | $C_{14}H_{18}O_{10}$ |
| 12 | Luteolin | 5280445 | $C_{15}H_{10}O_6$ |
| 13 | Lyoniresinol | 11711453 | $C_{22}H_{28}O_8$ |
| 14 | Quercetin-3-O-β-D-glucopyranoside | 12304324 | $C_{21}H_{20}O_{12}$ |

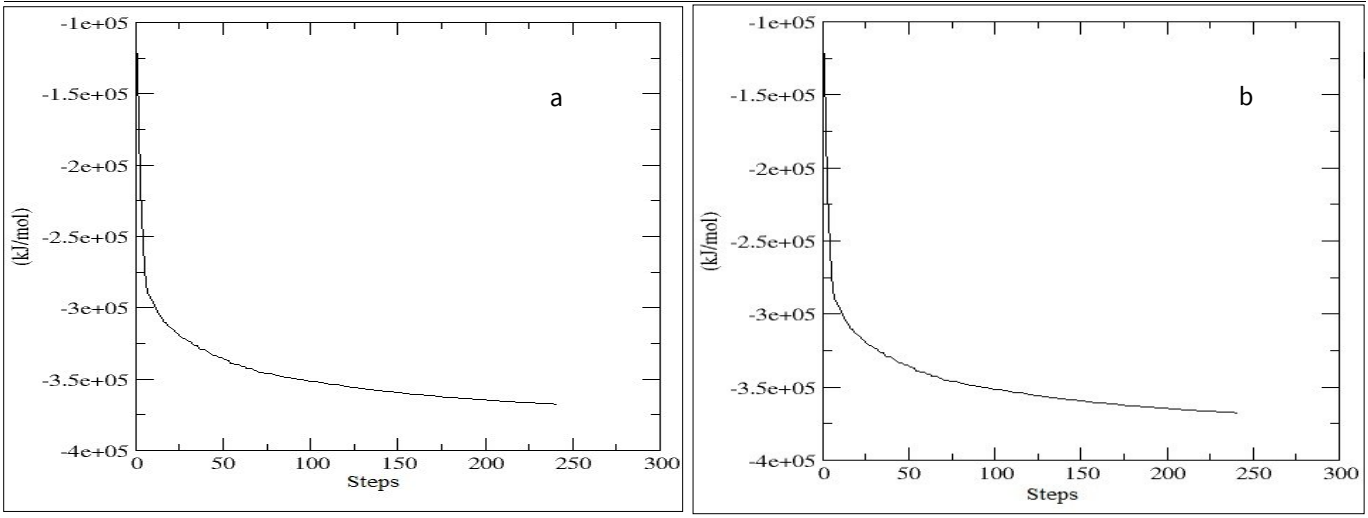


**Fig. 3.** Potential energy plots.

a) Lawsone; b) Caffeic acid complex with Nsp3 protein

Molecular Mechanics Poisson-Boltzmann Surface Area (MMPBSA) was employed to calculate the free energy of binding (△G) of complexes using g_mmpbsa tool of GROMACS (50). This can be calculated as:

$$\triangle G_{bind} = G_{complex} - (G_{protein}) + Gl_{igand}$$

## Results and Discussion

### Docking analysis of phytochemicals

For a good drug candidate, strong interactions with the protein are required (Fig. 4, Table 2) Negative energy values define a spontaneous interaction. More negative values indicate a strong binding affinity between protein-ligand complexes (40,51). The highest number of hydrogen bonds was shown by Luteolin-3-O-glucoside. Lawsone, was also seen to exhibit a high binding affinity of -7.4 kcal/mol.

### Phytochemical screening

The drug candidacy can be very easily comprehended by Lipinski's rule of 5, where lipophilicity (logP) of less than 5, less than 10 hydrogen bond acceptors, less than 5 hydrogen bond donors and a molecular mass of less than 500 Dalton, will increase the drug candidacy (Table 3). All the phytochemicals showed good performance, except chlorogenic acid, luteolin-3-O-glucoside, luteolin-7-O-β-D-glucopyranoside, quercetin-3-O-β-D-glucopyranoside and lalioside.

### *In silico* ADME analysis

Gastrointestinal absorption was good for all the phytochemicals except, rutin, luteolin-3-O-glucoside, chlorogenic acid and luteolin-7-O-β-D-glucopyranoside (Table 4). A score of >0.55 is considered good. Lawsone shows the highest bioactivity score, of 0.85, which is an indicator of the extent and rate at which the

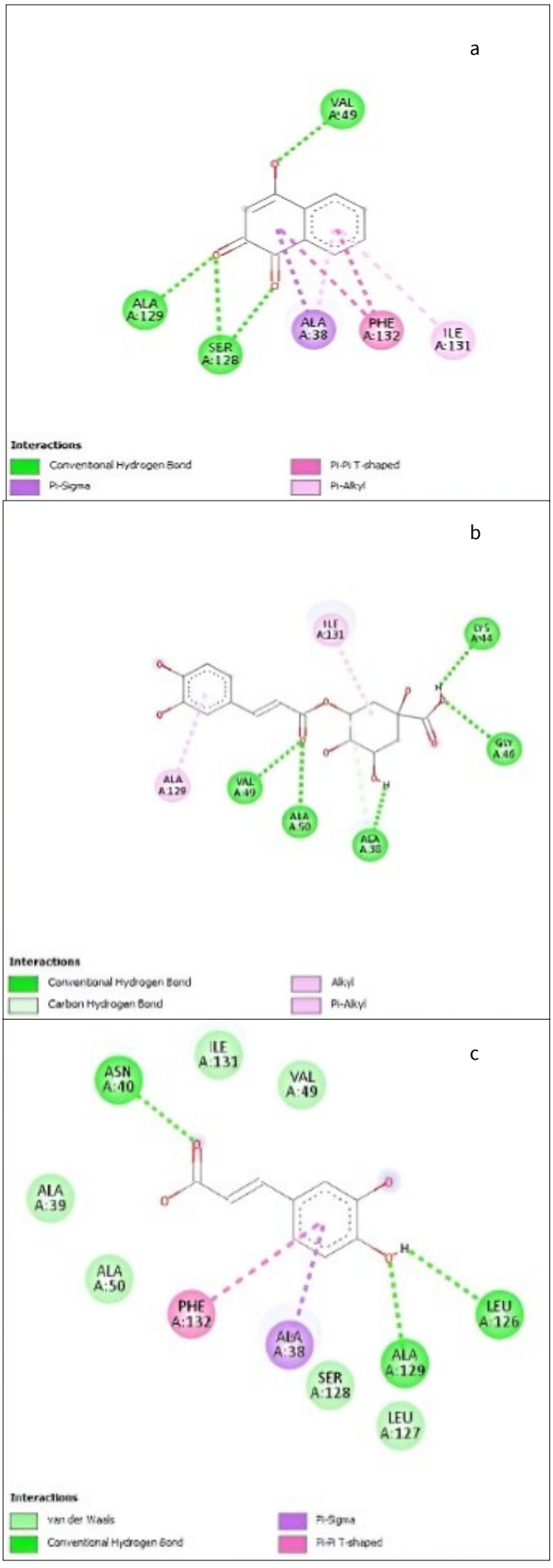
a
VAL A:49
ALA A:129
SER A:128
ALA A:38
PHE A:132
ILE A:131
Interactions
Conventional Hydrogen Bond
Pi-Sigma
Pi-Pi T-shaped
Pi-Alkyl
b
ILE A:131
LYS A:44
GLY A:46
ALA A:129
VAL A:49
ALA A:50
ALA A:38
Interactions
Conventional Hydrogen Bond
Carbon Hydrogen Bond
Alkyl
Pi-Alkyl
c
ILE A:131
ASN A:40
VAL A:49
ALA A:39
ALA A:50
PHE A:132
ALA A:38
SER A:128
ALA A:129
LEU A:126
LEU A:127
Interactions
van der Waals
Conventional Hydrogen Bond
Pi-Sigma
Pi-Pi T-shaped

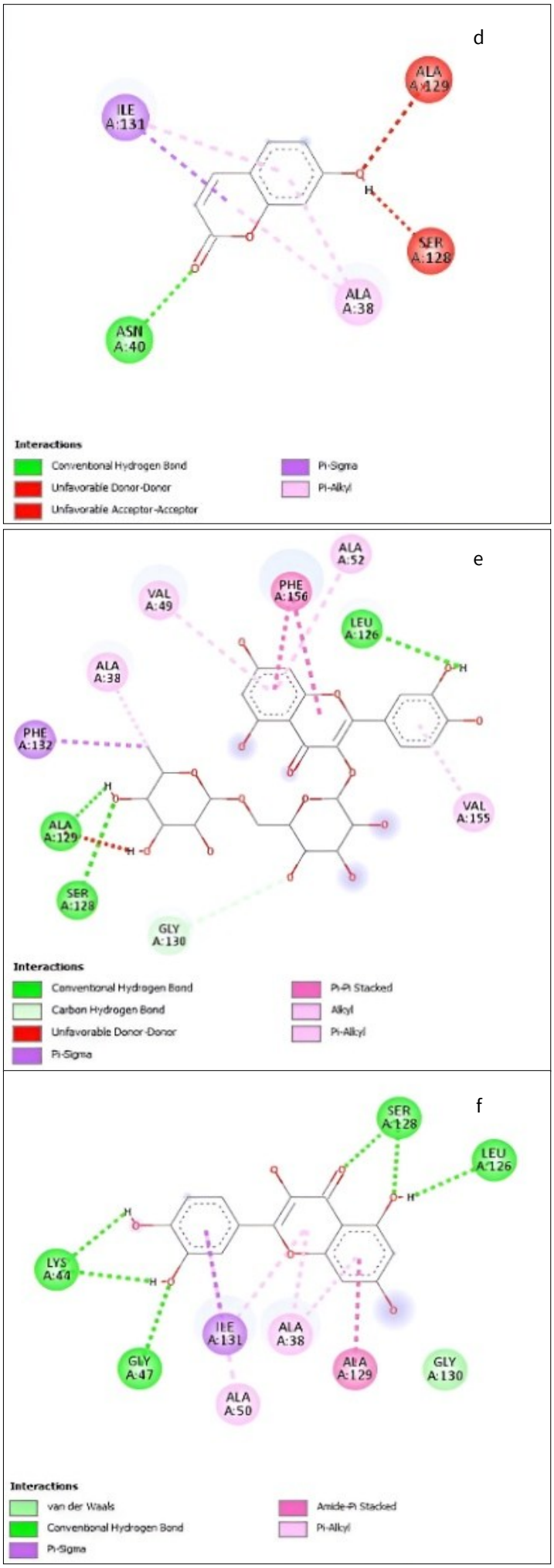
d
ALA A:129
ILE A:131
SER A:128
ALA A:38
ASN A:40
Interactions
Conventional Hydrogen Bond
Unfavorable Donor-Donor
Unfavorable Acceptor-Acceptor
Pi-Sigma
Pi-Alkyl
e
ALA A:52
PHE A:156
VAL A:49
LEU A:126
ALA A:38
PHE A:132
VAL A:155
ALA A:129
SER A:128
GLY A:130
Interactions
Conventional Hydrogen Bond
Carbon Hydrogen Bond
Unfavorable Donor-Donor
Pi-Sigma
Pi-Pi Stacked
Alkyl
Pi-Alkyl
f
SER A:128
LEU A:126
LYS A:44
ILE A:131
ALA A:38
GLY A:47
ALA A:129
GLY A:130
ALA A:50
Interactions
van der Waals
Conventional Hydrogen Bond
Pi-Sigma
Amide-Pi Stacked
Pi-Alkyl

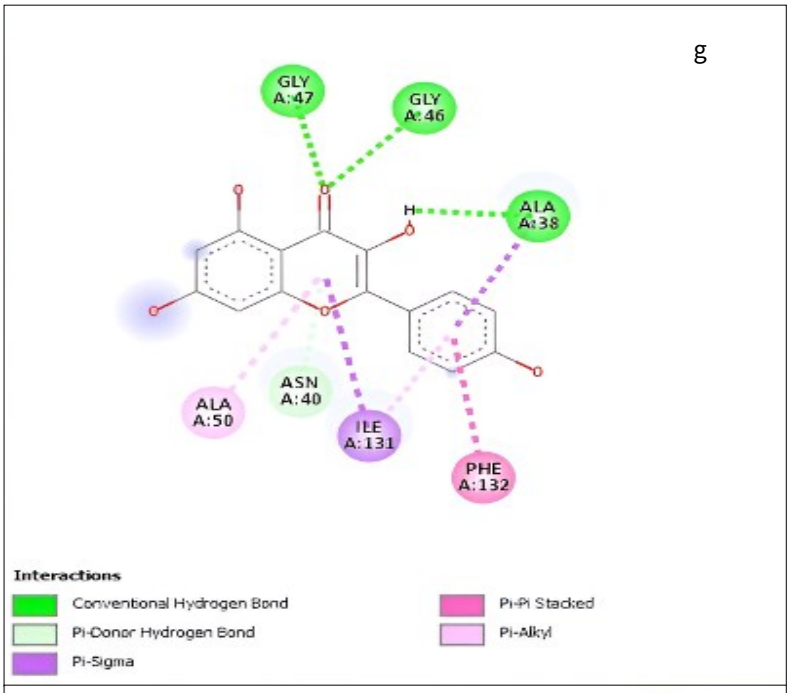
GLY A:47
GLY A:46
ALA A:38
ASN A:40
ALA A:50
ILE A:131
PHE A:132
Interactions
Conventional Hydrogen Bond
Pi-Donor Hydrogen Bond
Pi-Sigma
Pi-Pi Stacked
Pi-Alkyl

g

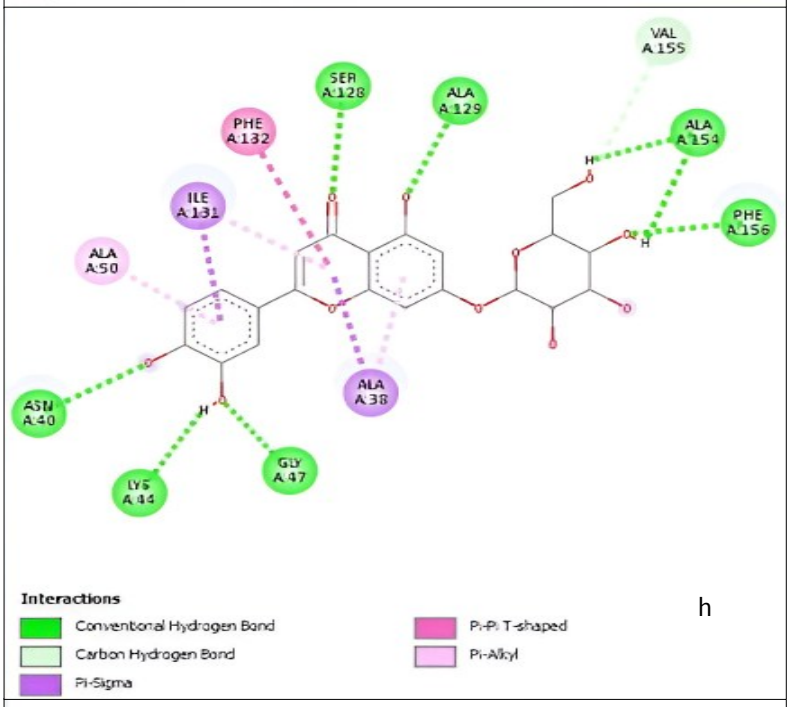
VAL A:155
SER A:128
ALA A:129
PHE A:132
ALA A:154
ILE A:131
PHE A:156
ALA A:50
ALA A:38
ASN A:40
LYS A:44
GLY A:47
Interactions
Conventional Hydrogen Bond
Carbon Hydrogen Bond
Pi-Sigma
Pi-Pi T-shaped
Pi-Alkyl

h

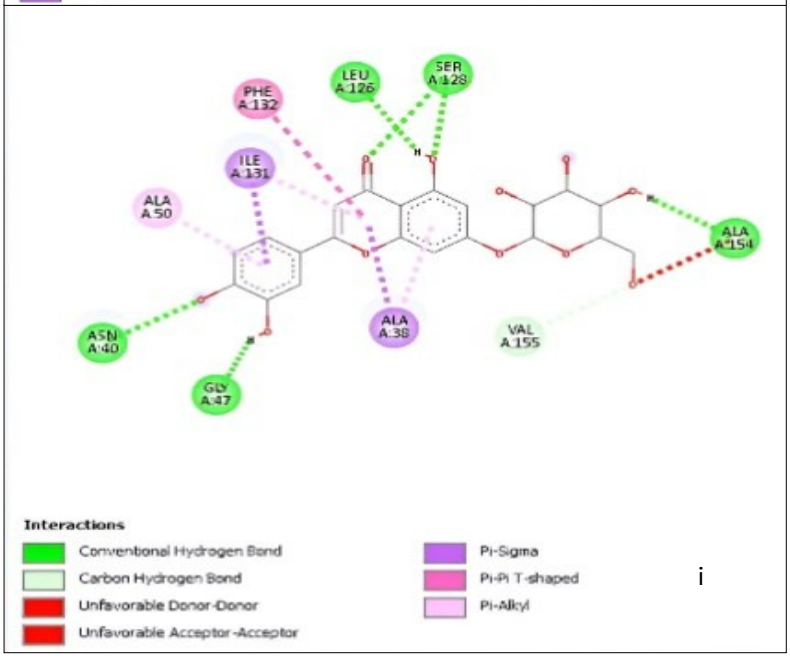
PHE A:132
LEU A:126
SER A:128
ILE A:131
ALA A:50
ALA A:154
ALA A:38
ASN A:40
VAL A:155
GLY A:47
Interactions
Conventional Hydrogen Bond
Carbon Hydrogen Bond
Unfavorable Donor-Donor
Unfavorable Acceptor-Acceptor
Pi-Sigma
Pi-Pi T-shaped
Pi-Alkyl

i

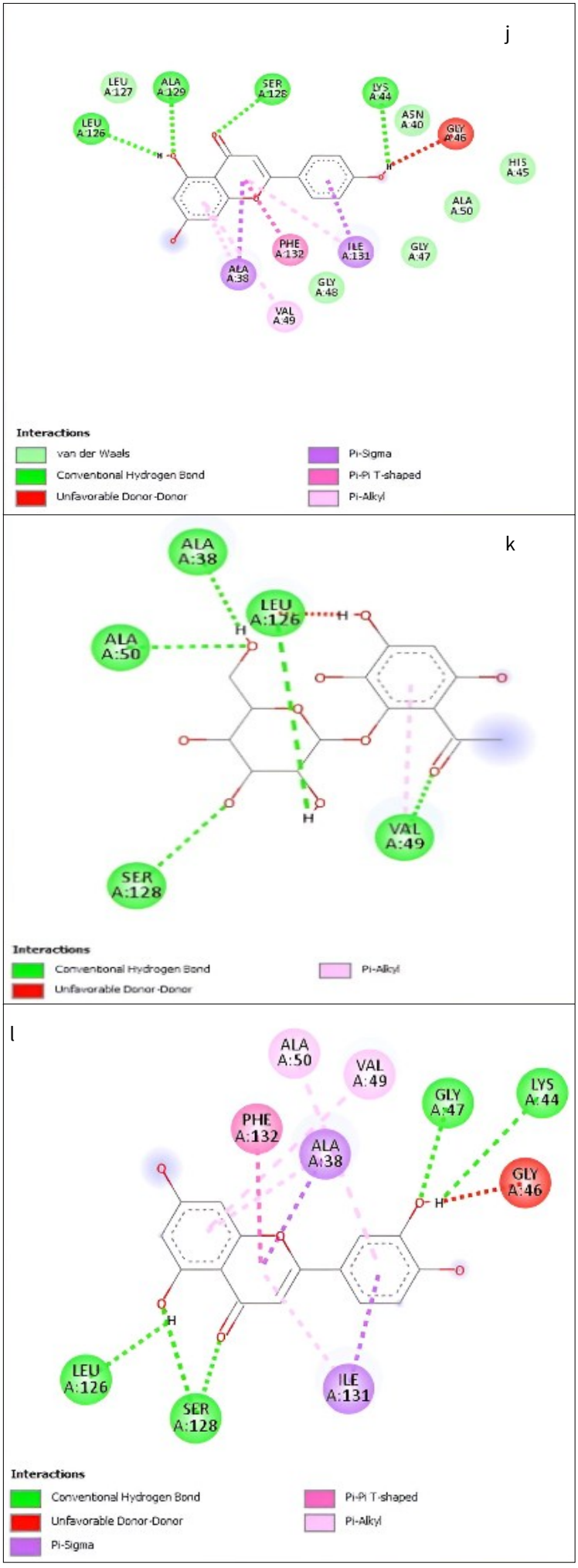
j
LEU A:127
ALA A:129
SER A:128
LYS A:44
ASN A:40
GLY A:46
LEU A:126
HIS A:45
ALA A:50
PHE A:132
ILE A:131
GLY A:47
ALA A:38
GLY A:48
VAL A:49
Interactions
van der Waals
Conventional Hydrogen Bond
Unfavorable Donor-Donor
Pi-Sigma
Pi-Pi T-shaped
Pi-Alkyl
k
ALA A:38
LEU A:126
ALA A:50
VAL A:49
SER A:128
Interactions
Conventional Hydrogen Bond
Unfavorable Donor-Donor
Pi-Alkyl
l
ALA A:50
VAL A:49
GLY A:47
LYS A:44
PHE A:132
ALA A:38
GLY A:46
LEU A:126
ILE A:131
SER A:128
Interactions
Conventional Hydrogen Bond
Unfavorable Donor-Donor
Pi-Sigma
Pi-Pi T-shaped
Pi-Alkyl

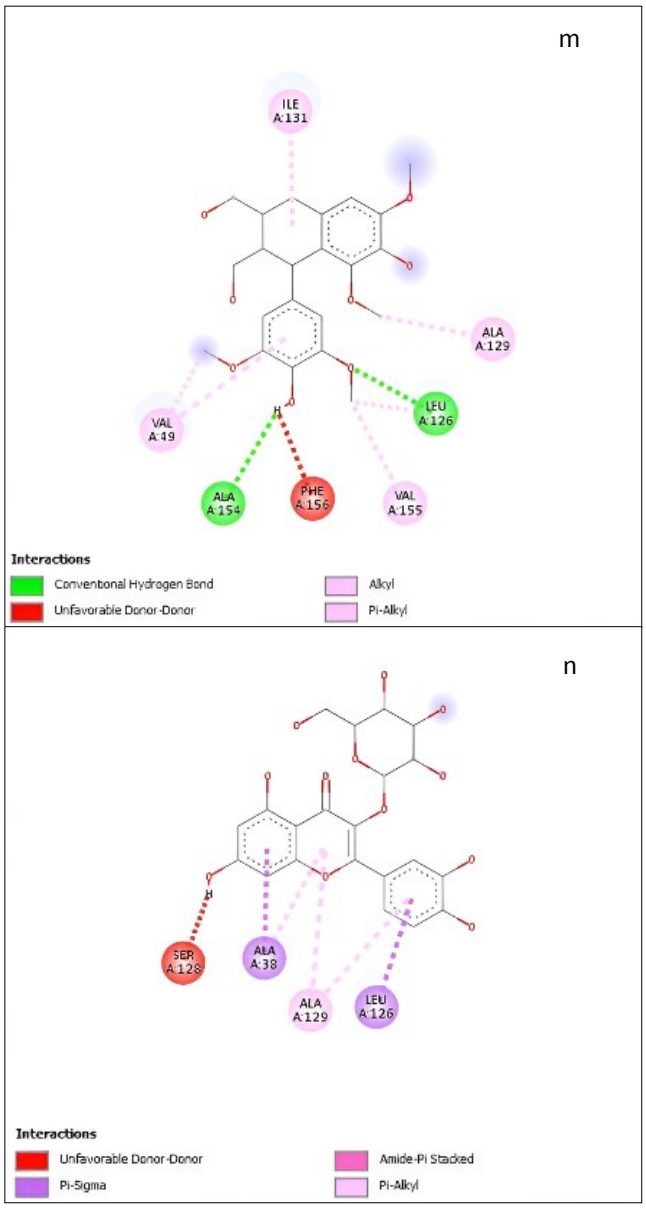


**Fig. 4**. Binding residues of protein Nsp3 with phytochemicals.

a) Lawsone; b) Chlorogenic acid; c) Caffeic acid; d) Umbelliferone; e) Rutin; f) Quercetin; g) Kaempferol; h) Luteolin-3-O-glucoside; i) Luteolin-7-O-β-D-glucopyranoside; j) Apigenin; k) Lalioside; l) Luteolin; m) Lyoniresinol; n) Quercetin-3-O-β-D-glucopyranoside

**Table 2**. Binding residues of phytochemicals with protein Nsp3

| Sr. No | Name | Binding affinity (kcal/mol) | H bonds | Binding residues |
|---|---|---|---|---|
| 1. | Lawsone | -7.4 | 4 | Ala 129 (A), Ser 128 (A), Val 49 (A) |
| 2. | Chlorogenic acid | -8.2 | 5 | Val 49 (A), Ala 50 (A), Ala 38 (A), Gly 46 (A), Lys 44 (A) |
| 3. | Caffeic acid | -7.0 | 3 | Ala 129 (A), Asn 40 (A), Leu 126 (A) |
| 4. | Umbelliferone | -6.7 | 1 | Asn 40 (A) |
| 5. | Rutin | -9.0 | 3 | Leu 126 (A), Ala 129 (A), Ser 128 (A) |
| 6. | Quercetin | -8.4 | 6 | Ser 128 (A), Leu 126 (A), Lys 44 (A), Gly 47 (A) |
| 7. | Kaempferol | -8.2 | 3 | Gly 46 (A), Gly 47 (A), Ala 38 (A) |
| 8. | Luteolin-3-O-glucoside | -10.0 | 8 | Ser 128 (A), Ala 129 (A), Ala 154 (A), Phe 156 (A), Gly 47 (A), Lys 44 (A), Asn 40 (A) |
| 9. | Luteolin-7-O-β-D-glucopyranoside | -10.0 | 6 | Leu 126 (A), Ser 128 (A), Ala 154 (A), Gly 47 (A), Asn 40 (A) |
| 10. | Apigenin | -8.7 | 4 | Leu 126 (A), Ala 129 (A), Ser 128 (A), Lys 44 (A), |
| 11. | Lalioside | -7.5 | 5 | Ala 38 (A), Ala 50 (A), Ser 128 (A), Leu 126 (A), Val 49 (A), |
| 12. | Luteolin | -8.9 | 5 | Leu 126 (A), Gly 47 (A), Ser 128 (A), Lys 44 (A), |
| 13. | Lyoniresinol | -6.5 | 2 | Ala 154 (A), Leu 126 (A) |
| 14. | Quercetin-3-O-β-D-glucopyranoside | -7.9 | - | - |

**Table 3**. Summary of ligands and their characters and violations to Lipinski's rule of 5

| SL. NO | Compound Name | Molecular Mass (g/mol) | H bond acceptors | H bond donors | LOG P | Molar refractivity | Violations |
|---|---|---|---|---|---|---|---|
| 1 | Lawsone | 174.15 | 3 | 1 | 0.83 | 46.39 | 0 |
| 2 | Chlorogenic acid | 354.31 | 9 | 6 | 0.96 | 83.50 | 1 |
| 3 | Caffeic acid | 180.16 | 4 | 3 | 0.97 | 47.16 | 0 |
| 4 | Umbelliferone | 162.14 | 3 | 1 | 1.44 | 44.51 | 0 |
| 5 | Rutin | 610.52 | 16 | 10 | 1.58 | 141.38 | 3 |
| 6 | Quercetin | 302.24 | 7 | 5 | 1.63 | 78.03 | 0 |
| 7 | Kaempferol | 286.24 | 6 | 4 | 1.70 | 76.01 | 0 |
| 8 | Luteolin-3-O-glucoside | 448.38 | 11 | 7 | 0.72 | 108.13 | 2 |
| 9 | Luteolin-7-O-β-D-glucopyranoside | 448.38 | 11 | 7 | 1.83 | 108.13 | 2 |
| 10 | Apigenin | 270.24 | 5 | 3 | 1.89 | 73.99 | 0 |
| 11 | Lalioside | 346.29 | 10 | 7 | 0.75 | 76.85 | 1 |
| 12 | Luteolin | 286.24 | 6 | 4 | 1.85 | 76.01 | 0 |
| 13 | Lyoniresinol | 420.45 | 8 | 4 | 2.92 | 110.31 | 0 |
| 14 | Quercetin-3-O-β-D-glucopyranoside | 464.38 | 12 | 8 | 2.11 | 110.16 | 2 |

**Table 4**. Analysis of phytochemicals using Swiss ADME analysis

| Name | LOG S | GIA | BBB | P-gp | CYP3A4 inhibitor | CYP1A2 inhibitor | Bioavailability score |
|---|---|---|---|---|---|---|---|
| Lawsone | -1.80 | High | Yes | No | No | No | 0.85 |
| Chlorogenic acid | -1.62 | Low | No | No | No | No | 0.11 |
| Caffeic acid | -1.89 | High | No | No | No | No | 0.56 |
| Umbelliferone | -2.46 | High | Yes | No | No | Yes | 0.55 |
| Rutin | -3.30 | Low | No | Yes | No | No | 0.17 |
| Quercetin | -3.16 | High | No | No | Yes | Yes | 0.55 |
| Kaempferol | -3.31 | High | No | No | Yes | Yes | 0.55 |
| Luteolin-3-O-glucoside | -3.65 | Low | No | No | No | No | 0.17 |
| Luteolin-7-O-β-D-glucopyranoside | -3.65 | Low | No | Yes | No | No | 0.17 |
| Apigenin | -3.94 | High | No | No | Yes | Yes | 0.55 |
| Lalioside | -1.23 | Low | No | No | No | No | 0.55 |
| Luteolin | -3.71 | High | No | No | Yes | Yes | 0.55 |
| Lyoniresinol | -3.53 | High | No | Yes | No | No | 0.55 |
| Quercetin-3-O-β-D-glucopyranoside | -3.04 | Low | No | No | No | No | 0.17 |

ligand enters the system, accessing the site of action. Ligands that are p-glycoprotein substrates, can substantially reduce drug metabolism, hence are not acceptable. CYP enzymes are very important for drug absorption and metabolism, inhibitors of which, are discouraged. Quercetin, kaempferol, apigenin and luteolin don't satisfy the criteria, whereas lawsone and caffeic acid, can serve as prospective drug candidates that qualify the screening parameters successfully.

## Bioactivity score

The phytochemicals showed a high to moderate bioactivity score, apart from umbelliferone, which showed lowest score in kinase Inhibition of -1.30. For G protein-coupled receptor (GPCR), Ion channel modulator (ICM), Enzyme inhibitor (EI), Protease inhibitor (PI) and Nuclear receptor ligand (NRL), high bioactivity score was shown by chlorogenic acid (Table 5).

## AMDET analysis

All 14 phytochemicals were tested for ADME and toxicity to further screen the compound's candidature as effective drugs (Table 6). Regarding the absorption parameters, all phytochemicals showed optimal values. The distribution result showed that the compounds are well distributed in tissue. All compounds also showed a good renal elimination by not being renal organic cation transporter 2 (OCT2) substrates. AMES toxicity was not shown for the selected compound list. Only umbelliferone showed hepatotoxicity. Comparing all the parameters, lawsone and caffeic acid showed best results among the ligands.

## Molecular Dynamic (MD) simulations

A dynamic interaction between the complexes can be understood by MD simulations. Docking methods give a stringent view, which can be easily overcome by simulation studies (45). These simulation studies also help in making the process of drug discovery less time

**Table 5**. Bioactivity score of the phytochemicals with the Molinspiration software

| SL. NO | Name | GPCR | ICM | KI | NRL | PI | EI |
|---|---|---|---|---|---|---|---|
| 1 | Lawsone | -0.76 | -0.13 | -0.41 | -0.86 | -0.74 | 0.20 |
| 2 | Chlorogenic acid | 0.29 | 0.14 | -0.00 | 0.74 | 0.27 | 0.62 |
| 3 | Caffeic acid | -0.48 | -0.23 | -0.81 | -0.10 | -0.79 | -0.09 |
| 4 | Umbelliferone | -1.22 | -0.72 | -1.30 | -0.92 | -1.30 | -0.35 |
| 5 | Rutin | -0.05 | -0.52 | -0.14 | -0.23 | -0.07 | 0.12 |
| 6 | Quercetin | 0.06 | -0.19 | 0.28 | 0.36 | -0.25 | 0.28 |
| 7 | Kaempferol | -0.10 | -0.21 | 0.21 | 0.32 | -0.27 | 0.26 |
| 8 | Luteolin-3-O-glucoside | 0.10 | -0.01 | 0.18 | 0.28 | -0.02 | 0.43 |
| 9 | Luteolin-7-O-β-D-glucopyranoside | 0.09 | -0.02 | 0.15 | 0.27 | -0.01 | 0.42 |
| 10 | Apigenin | -0.07 | -0.09 | 0.18 | 0.34 | -0.25 | 0.26 |
| 11 | Lalioside | 0.03 | 0.06 | -0.14 | 0.07 | -0.01 | 0.38 |
| 12 | Luteolin | -0.02 | -0.07 | 0.26 | 0.39 | -0.22 | 0.28 |
| 13 | Lyoniresinol | 0.07 | 0.00 | -0.18 | -0.05 | -0.02 | 0.10 |
| 14 | Quercetin-3-O-β-D-glucopyranoside | 0.06 | -0.04 | 0.13 | 0.20 | -0.06 | 0.42 |

**Table 6**. ADMET prediction of the phytochemicals

| Sl.NO | MOLECULE | Absorption | | | Distribution | | | Excretion | | | Toxicity | | | | | |
|---|---|---|---|---|---|---|---|---|---|---|---|---|---|---|---|---|
| | | $Caco_2$ | HIA | Skin | VDss | FU | BBB | CNS | TC | Renal OCT2 | AMES | MTDD | hERG I | hERG II | LD50 | HT | SS | MT |
| 1. | Lawsone | 1.19 | 93.8 | -3.04 | 0.01 | 0.01 | -0.23 | -2.79 | 0.15 | No | No | 0.97 | No | No | 1.82 | No | No | 1.57 |
| 2 | Chlorogenic acid | -0.84 | 36.4 | -2.74 | 0.58 | 0.66 | -1.41 | -3.86 | 0.30 | No | No | -0.13 | No | No | 1.97 | No | No | 5.74 |
| 3 | Caffeic acid | 0.63 | 69.4 | -2.72 | -1.09 | 0.53 | -0.65 | -2.61 | 0.50 | NO | NO | 1.14 | No | No | 2.38 | No | No | 2.24 |
| 4 | Umbelliferone | 1.21 | 94.5 | -2.6 | 0.03 | 0.43 | -0.28 | -2.74 | 0.70 | No | No | 0.68 | No | No | 2.04 | Yes | No | 1.71 |
| 5 | Rutin | -0.95 | 23.4 | -2.74 | 1.66 | 0.18 | -1.89 | -5.18 | -0.37 | NO | NO | 0.45 | No | Yes | 2.49 | No | No | 7.67 |
| 6 | Quercetin | -0.23 | 77.2 | -2.74 | 1.56 | 0.20 | -1.09 | -3.06 | 0.49 | NO | NO | 0.49 | No | No | 2.47 | No | No | 3.72 |
| 7 | Kaempferol | 0.03 | 74.2 | -2.74 | 1.27 | 0.17 | -0.94 | -2.23 | 0.47 | No | No | 0.53 | No | No | 2.44 | No | No | 2.88 |
| 8 | Luteolin-3-O-glucoside | 0.28 | 30.3 | -2.74 | 1.35 | 1.35 | -1.63 | -3.91 | 0.47 | No | No | 0.58 | No | No | 2.54 | No | No | 5.94 |
| 9 | Luteolin-7-O-β-D glucopyranoside | 0.24 | 37.5 | -2.73 | 0.88 | 0.22 | -1.56 | -3.93 | 0.47 | No | No | 0.58 | No | No | 2.54 | No | No | 6.34 |
| 10 | Apigenin | 1.00 | 93.2 | -2.73 | 0.82 | 0.15 | -0.73 | -2.06 | 0.56 | No | No | 0.32 | No | No | 2.45 | No | No | 2.43 |
| 11 | Lalioside | -0.86 | 24.2 | -2.73 | 0.80 | 0.71 | -1.49 | -4.14 | 0.52 | No | No | 0.24 | No | No | 2.40 | No | No | 6.88 |
| 12 | Luteolin | 0.09 | 81.1 | -2.73 | 1.15 | 0.17 | -0.91 | -2.25 | 0.49 | No | No | 0.49 | No | No | 2.45 | No | No | 3.16 |
| 13 | Lyoniresinol | -0.27 | 72.2 | -2.73 | 0.19 | 0.05 | -1.11 | -1.11 | 0.37 | No | No | 0.41 | No | Yes | 2.08 | No | No | 2.46 |
| 14. | Quercetin-3-O-β-D-glucopyranoside | 0.24 | 47.9 | -2.73 | 1.84 | 0.23 | -1.68 | -4.04 | 0.39 | No | No | 0.56 | No | Yes | 2.54 | No | No | 8.06 |

consuming for the industry (52). We performed simulations for the best ligand-protein complexes, as was evident by previous screening analysis, (lawsone-Nsp3 and caffeic acid-Nsp3), for 100 ns, to finally select the best candidate.

## Root Mean Square Deviation (RMSD)

We can say that Lawsone-Nsp3 and Caffeic acid-Nsp3 show very low RMSD, within 0.1-0.15 nm, (expected and stable range is 0.1-0.7nm with respect to size of the protein) till 100 ns. RMSD values also show that the variation is insignificant in terms of its structure which indicates a high stability (53) (Fig. 5). For the excellent category, RMSD values need to be less than 0.05 nm (54). Hence, lawsone and caffeic acid can serve as potential good hits based on their very low RMSD values.

## Root Mean Square Fluctuation (RMSF)

From the results, the RMSF observed range is less than 0.3 nm for caffeic acid and lawsone complexes, indicating no significant change in the structure of protein-ligand complexes, suggesting strong and compact complexes (Fig. 6). Glycine and aspartic acid residues show highest mobility, contributing to protein flexibility.

## Radius of gyration radius of gyration (Rg)

The radius of gyration measures protein and ligand compactness, throwing light on the folding properties of the protein (55,56). Small values indicate a compact complex. High Rg values indicate unstable protein folding and complexes (57). A stable value of the radius of gyration indicates stable protein folding. Analysis shows that the radius of gyration is relatively stable for both the Lawsone-Nsp3 and Caffeic acid-Nsp3 complexes. The stable graph (black colour) shows that the protein can maintain its compactness (Fig. 7).

## Thermodynamic properties of the system

To calculate the free energy of binding (△G) of complexes, MMPBSA was employed (Table 7). MMPBSA calculated the various forces (Table 7) for both complexes. Both complexes remain stable for 100 ns. It was found that the binding energy for 'caffeic acid' is -16.32 kcal/mol, while -20.72 kcal/mol for the 'lawsone'. These energies represent stronger binding for lawsone. In addition, energy less than -7 kcal/mol shows stronger binding. The complex 'Lawsone' is more stable than the 'Caffeic acid' based on lower free energy.

The medicinal importance of *Lawsonia inermis* is well established, given the rich secondary metabolites (9). When it comes to plant-based phytochemicals, we usually see flavonoids as effective antiviral agents, like diosmin (58–60). This analysis, however, show that, between caffeic acid and lawsone, a naphthoquinone, which is also the main pigment, emerging as a potential antiviral candidate (61,62). Naphthoquinones are derivatives of the shikimic acid pathway and have well established medicinal benefits (63,64). Earlier studies reveal the effective role of liposome-encapsulated derivatives of naphthoquinones in inhibiting HSV infection (65). Even novel derivatives of 1,4-naphthoquinones have shown effective antimicrobial functions (66). 3,5,8-trihydroxy-6-methoxy-2-(5-oxohexa-1,3-dienyl)-naphthanthene-1,4-dione, a naphthoquinone produced by a fungus was reported to reduce inflammation and inhibit transcription (hindering the virus pathogenicity) in SARS-CoV-2 infected cells (67). From our study, it was interesting to see that, for the very first time, between caffeic acid and lawsone, lawsone yielded the best results, against Nsp3 protein. Naphthoquinones achieve the antiviral property mainly by inhibiting the $Na^+$, $K^+$-

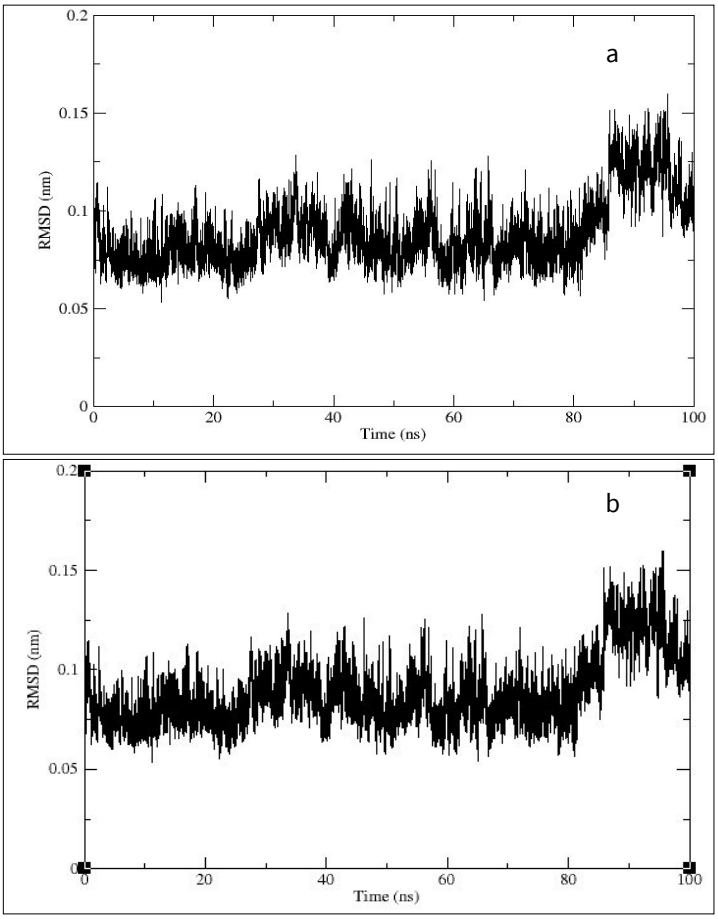


**Fig. 5.** RMSD plots.

a) Lawsone; b) caffeic acid complex with protein Nsp3

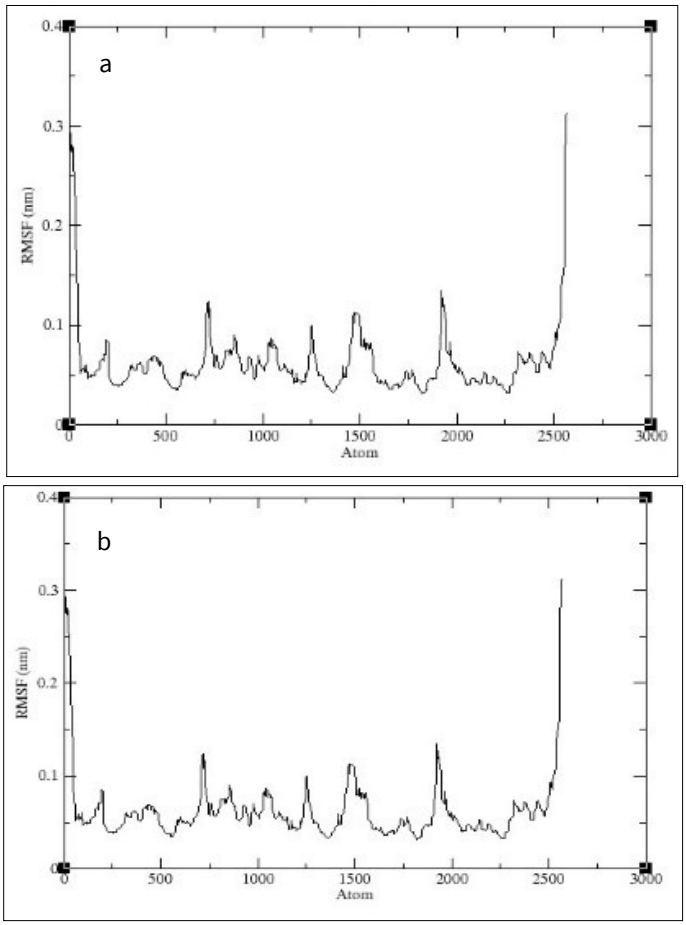


**Fig. 6**. RMSF plots.

a) Lawsone; b) caffeic acid complex with protein Nsp3

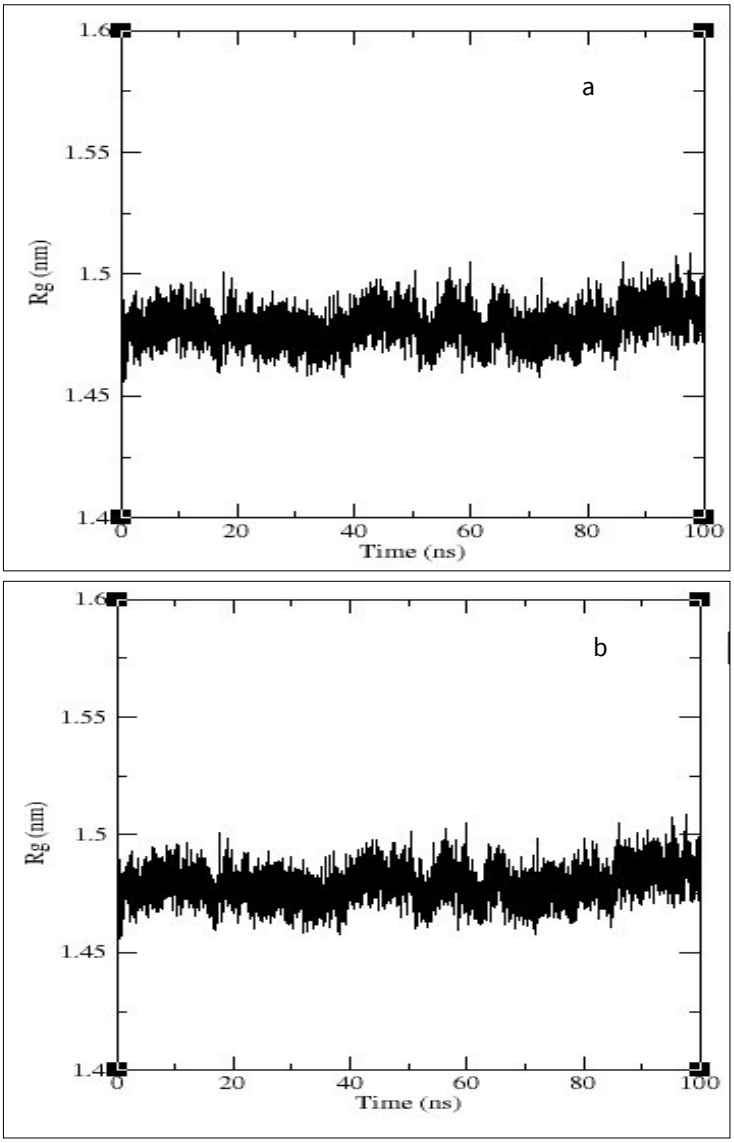


**Fig. 7.** Radius of gyration (Rg) plots.

a) Lawsone; b) caffeic acid complex with protein Nsp3

**Table 7**. Energies of the complexes

| S.No | Complex | Vanderwaal energy (kcal/mol) | Electrostatic energy (kcal/mol) | Polar and Non Polar solvation energy (kcal/mol) | SASA energy (kcal/mol) | Free Binding energy (kcal/mol) |
|---|---|---|---|---|---|---|
| 1 | Lawsone-Nsp3 | -1155.92 | -11392.83 | -1904.39 | 65.02 | -20.72 |
| 2 | Caffeic Acid-Nsp3 | -1149.59 | -11394.57 | -1917.29 | 66.26 | -16.32 |

ATPase and by interfering with the steps of attachment and penetration of the virus (65,68,69).

The importance of the Nsp3 protein lies in its many functions to ensure the survival of the virus, by promoting of replication, transcription and translation (26,27,29,32,70). A triterpene glycoside, suavissimoside, was reported to hinder the activity SARS-CoV $M^{Pro}$, having a binding energy of -8.19 kcal/mol (71). Sulfuretin, was also reported to show good binding results with Nsp3 (72). Chlorogenic acid from *Lawsonia inermis* also showed effective binding and interaction with NS1 of Dengue virus (15), with a binding energy of -43.39 kJ/mol. In this study, we see the main pigment of the plant, lawsone, to be effective against Nsp3. No previous studies were found, that explored the interactions of lawsone against Nsp3, proving the uniqueness of the analysis. Lawsone and caffeic acid satisfied most of the screening tests, which were further simulated for a time of 100 ns, by MD simulations. Analysis of RMSD, RMSF and Rg showed the ligand-protein complexes, analysing which, concluded strong and compact complexes. Binding free energy for the complex lawsone was -20.72 kcal/mol, suggesting favourable energy parameters as compared to caffeic acid complex. From the results it is clear that the Lawsone-Nsp3 complex is more stable. This analysis shows better binding affinity as compared to suavissimoside to SARS-CoV $M^{pro}$, with an affinity of -8.19 kcal/mol (71). This was similar to the energy of a few best docked ligands against Nsp3, showing an affinity of more than -8.5 kcal/mol (73). When comparing with previous works (74,75) ligand binding affinity was seen to be higher for our analysis, where the ligands interacted with the inhibitory binding residues of Nsp3 protein.

Our analysis yielded better results, showing the possibility of a natural dying agent, as a potential antiviral compound. This analysis also highlights the interactions of lawsone, a naphthoquinone, against Nsp3 protein. In hindsight, this work can successfully establish the plant in the medicinal sector.

## Conclusion

We can conclude from the analysis that a naphthoquinone, lawsone, which is the main pigment of the plant, can serve as a potential candidate against Nsp3 protein of SARS-CoV2, providing a plant-based alternative that can successfully bind and inhibit the protein, needed for protein processing by the virus. Further isolation of lawsone and application in *in vitro* methods, can strengthen the candidature of the ligand against the protein's functions.


## Acknowledgements

The authors are grateful to the West Bengal Department of Higher Education of Science and Technology and Biotechnology, Department of Biotechnology (DBT) and Department of Science and Technology (DST) for financially aiding the research.


## Authors' contributions

DD and DS wrote paper, collected data and analysed data. DR, SD and BM designed research and edited the manuscript. All authors read and approved the final manuscript.

## Compliance with ethical standards

**Conflict of interest:** Authors do not have any conflict of interests to declare.

**Ethical issues:** None

## References


1. Kala CP, Dhyani PP, Sajwan BS. Developing the medicinal plants sector in northern India: challenges and opportunities. J Ethnobiol Ethnomed. 2006;2:32. https://doi.org/10.1186/1746-4269-2-32
2. Fokunang CN, Ndikum V, Tabi OY, Jiofack RB, Ngameni B, Guedje NM, et al. Traditional medicine: past, present and future research and development prospects and integration in the national health system of Cameroon. Afr J Tradit Complement Altern Med. 2011;8 (3):284-95. https://doi.org/10.4314/ajtcam.v8i3.65276
3. Alzaabi MM, Hamdy R, Ashmawy NS, Hamoda AM, Alkhayat F, Khademi NN, et al. Flavonoids are promising safe therapy against COVID-19. Phytochem Rev. 2022;21(1):291-312.https://doi.org/10.1007/s11101-021-09759-z
4. Ravishankar B, Shukla VJ. Indian systems of medicine: a brief profile. Afr J Tradit Complement Altern Med. 2007;4(3):319-37. https://doi.org/10.4314/ajtcam.v4i3.31226
5. Viale M, Vicol M. Conserving traditional wisdom in a commodified landscape: unpacking brand Ayurveda. J Ayurveda Integr Med. 2023;14(1):100667. https://doi.org/10.1016/j.jaim.2022.100667
6. Kumar S, Dobos GJ, Rampp T. The significance of Ayurvedic medicinal plants. Evid Based Complement Alternat Med. 2016;22 (3):494-501. https://doi.org/10.1177/2156587216671392
7. Kudlu C. Keeping the doctor in the loop: Ayurvedic pharmaceuticals in Kerala. Anthropol Med. 2016;23(3):275-94.https://doi.org/10.1080/13648470.2016.1181520
8. Chaudhary G, Goyal S, Poonia P. *Lawsonia inermis* Linnaeus: a phytopharmacological review. Int J Pharm Sci Drug Res. 2010;2 (2):91-8. https://doi.org/10.25004/IJPSDR.2010.020202
9. Adiga A, Gandhi A, Pradeep P, Hegde L. Comprehensive review on Madayantika (*Lawsonia inermis* L.). J Ayurveda Integr Med Sci. 2022;7(10):204-10.
10. Badoni Semwal R, Semwal DK, Combrinck S, Cartwright-Jones C, Viljoen A. *Lawsonia inermis* L. (henna): ethnobotanical, phytochemical and pharmacological aspects. J Ethnopharmacol. 2014;155(1):80-103. https://doi.org/10.1016/j.jep.2014.05.042
11. Singh D, Luqman S. *Lawsonia inermis* (L.): a perspective on anticancer potential of mehndi/henna. Biomed Res Ther. 2014;1 (4):112-20. https://doi.org/10.7603/s40730-014-0018-1
12. Ponugoti M. A pharmacological and toxicological review of *Lawsonia inermis*. Int J Pharm Sci Res. 2018;9(3):902-15.
13. Tungmunnithum D, Thongboonyou A, Pholboon A, Yangsabai A. Flavonoids and other phenolic compounds from medicinal plants for pharmaceutical and medical aspects: an overview. Medicines (Basel). 2018;5(3):93. https://doi.org/10.3390/medicines5030093
14. Ekor M. The growing use of herbal medicines: issues relating to adverse reactions and challenges in monitoring safety. Front Pharmacol. 2014;4:177. https://doi.org/10.3389/fphar.2013.00177
15. Das D, Mallick B, Sinha S, Ganguli S, Samanta D, Banerjee R, et al. Unearthing the inhibitory potential of phytochemicals from *Lawsonia inermis* L. and some drugs against dengue virus protein NS1: an *in silico* approach. J Biomol Struct Dyn. 2023;29:1-18. https://doi.org/10.1080/07391102.2023.2298730
16. Dhamanti I, Suwantika AA, Adlia A, Yamani LN, Yakub F. Adverse reactions of COVID-19 vaccines: a scoping review of observational studies. Int J Gen Med. 2023;16:609-18. https://doi.org/10.2147/IJGM.S400458
17. Rabail R, Ahmed W, Ilyas M, Rajoka MSR, Hassoun A, Khalid AR, et al. The side effects and adverse clinical cases reported after COVID-19 immunization. Vaccines. 2022;10(4):488. https://doi.org/10.3390/vaccines10040488
18. El Sayed KA. Natural products as antiviral agents. Stud Nat Prod Chem. 2000;24:473-572. https://doi.org/10.1016/S1572-5995(00)80051-4
19. Badshah SL, Faisal S, Muhammad A, Poulson BG, Emwas AH, Jaremko M. Antiviral activities of flavonoids. Biomed Pharmacother. 2021;140:111596. https://doi.org/10.1016/j.biopha.2021.111596
20. Ben-Shabat S, Yarmolinsky L, Porat D, Dahan A. Antiviral effect of phytochemicals from medicinal plants: applications and drug delivery strategies. Drug Deliv Transl Res. 2020;10(2):354-67. https://doi.org/10.1007/s13346-019-00691-6
21. Loaiza-Cano V, Monsalve-Escudero LM, da Silva Maia Bezerra Filho C, Martinez-Gutierrez M, De Sousa DP. Antiviral role of phenolic compounds against dengue virus: a review. Biomolecules. 2020;11 (1):11. https://doi.org/10.3390/biom11010011
22. Montenegro-Landívar MF, Tapia-Quirós P, Vecino X, Reig M, Valderrama C, Granados M, et al. Polyphenols and their potential role to fight viral diseases: an overview. Sci Total Environ. 2021;801:149719. https://doi.org/10.1016/j.scitotenv.2021.149719
23. Khalil A, Tazeddinova D. The upshot of polyphenolic compounds on immunity amid COVID-19 pandemic and other emerging communicable diseases: an appraisal. Nat Prod Bioprospect. 2020;10(6):411-29. https://doi.org/10.1007/s13659-020-00271-z
24. Batiha GE, Teibo JO, Shaheen HM, Babalola BA, Teibo TKA, Al-Kuraishy HM, et al. Therapeutic potential of *Lawsonia inermis* Linn: a comprehensive overview. Naunyn Schmiedebergs Arch Pharmacol. 2024;397(6):3525-40. https://doi.org/10.1007/s00210-023-02735-8
25. Armstrong LA, Lange SM, Dee Cesare V, Matthews SP, Nirujogi RS, Cole I, et al. Biochemical characterization of protease activity of Nsp3 from SARS-CoV-2 and its inhibition by nanobodies. PLoS One. 2021;16(7):e0253364. https://doi.org/10.1371/journal.pone.0253364
26. Angelini MM, Akhlaghpour M, Neuman BW, Buchmeier MJ. Severe acute respiratory syndrome coronavirus non-structural proteins 3, 4 and 6 induce double-membrane vesicles. mBio. 2013;4(4):e00524-13. https://doi.org/10.1128/mBio.00524-13
27. Lei J, Kusov Y, Hilgenfeld R. Nsp3 of coronaviruses: structures and functions of a large multi-domain protein. Antiv Res. 2018;149:58-74. https://doi.org/10.1016/j.antiviral.2017.11.001

28. Bills C, Xie X, Shi P. The multiple roles of nsp6 in the molecular pathogenesis of SARS-CoV-2. Antivir Res. 2023;213:105590. https://doi.org/10.1016/j.antiviral.2023.105590

29. Osipiuk J, Azizi SA, Dvorkin S, Endres M, Jedrzejczak R, Jones KA, et al. Structure of papain-like protease from SARS-CoV-2 and its complexes with non-covalent inhibitors. Nat Commun. 2021;12 (1):743. https://doi.org/10.1038/s41467-021-21060-3

30. Majiya H, Galstyan A. Potential of a methanolic extract of *Lawsonia inermis* (L.) leaf as an alternative sanitiser in the time of COVID-19 pandemic and beyond. J Herb Med. 2023;38:100633. https://doi.org/10.1016/j.hermed.2023.100633

31. Jamal QMS. Antiviral potential of plants against COVID-19 during outbreaks-an update. Int J Mol Sci. 2022;23(21):13564. https://doi.org/10.3390/ijms232113564

32. Li Y, Pustovalova Y, Shi W, Gorbatyuk O, Sreeramulu S, Schwalbe H, et al. Crystal structure of the CoV-Y domain of SARS-CoV-2 non-structural protein 3. Sci Rep. 2023;13:2890. https://doi.org/10.1038/s41598-023-30045-9

33. Golwala DK, Vaidya SK, Patel TB, Patel DS, Dholwani KK. Phytochemical and antioxidant activities of methanolic extract of *Lawsonia inermis* L. bark. Curr Issues Pharm Med Sci. 2020;33(3):132 -8. https://doi.org/10.2478/cipms-2020-0024

34. Paul D, Surendran S, Chandrakala P, Satheeshkumar N. An assessment of the impact of green tea extract on palbociclib pharmacokinetics using a validated UHPLC-QTOF-MS method. Biomed Chromatogr. 2019;33 (4):e4469.https://doi.org/10.1002/bmc.4469

35. Das D, Samanta D, Banerjee R, Sinha S, Mallick B, Ganguli S, et al. Insights into the phytochemical potential of *Lawsonia inermis* L. for future small molecule based therapeutic applications. Int Res J Plant Sci. 2020;11:1-7.

36. Shim H, Kim H, Allen JE, Wulff H. Pose classification using three-dimensional atomic structure-based neural networks applied to ion channel-ligand docking. J Chem Inf Model. 2022;62(10):2301-15. https://doi.org/10.1021/acs.jcim.1c01510

37. Bultum LE, Tolossa GB, Lee D. Combining empirical knowledge, in silico molecular docking and ADMET profiling to identify therapeutic phytochemicals from *Brucea antidysentrica* for acute myeloid leukemia. PLoS One. 2022;17(7):e0270050. https://doi.org/10.1371/journal.pone.0270050

38. Daina A, Michielin O, Zoete V. SwissADME: a free web tool to evaluate pharmacokinetics, drug-likeness and medicinal chemistry friendliness of small molecules. Sci Rep. 2017;7(1):42717. https://doi.org/10.1038/srep42717

39. Sączewski J, Popenda Ł, Fedorowicz J. In silico SwissADME analysis of antibacterial NHC-silver acetates and halides complexes. Appl Sci. 2024;14(19):8865. https://doi.org/10.3390/app14198865

40. Shruti Y, Prabhudev SM, Channamma M, Hanamanth JK, Singh KC. Drug likeliness, bioavailability, virtual screening and docking studies of some sulphonamide derivatives. WJPR. 2023;12(13):1094-1107.

41. Stefaniu A, Pirvu LC. In silico study approach on a series of 50 polyphenolic compounds in plants; a comparison on the bioavailability and bioactivity data. Molecules. 2022;27(4):1413. https://doi.org/10.3390/molecules27041413

42. Guan L, Yang H, Cai Y, Sun L, Di P, Li W, et al. ADMET-score - a comprehensive scoring function for evaluation of chemical drug likeness. Med Chem Commun. 2018;10(1):148-57. https://doi.org/10.1039/C8MD00472B

43. Cheng F, Li W, Liu G, Tang Y. In silico ADMET prediction: recent advances, current challenges and future trends. Curr Top Med Chem. 2013;13 (11):1273-89. https://doi.org/10.2174/15680266113139990033

44. Trott O, Olson AJ. AutoDock Vina: improving the speed and accuracy of docking with a new scoring function, efficient optimization and multithreading. J Comput Chem. 2009;31(2):455-61.https://doi.org/10.1002/jcc.21334

45. Karplus M, McCammon J. Molecular dynamics simulations of biomolecules. Nat Struct Mol Biol. 2002;9(9):646-52. https://doi.org/10.1038/nsb0902-646

46. Hospital A, Goni JR, Orozco M, Gelpi JL. Molecular dynamics simulations: advances and applications. Adv Appl Bioinform Chem. 2015;8:37-47. https://doi.org/10.2147/AABC.S70333

47. Kutzner C, Kniep C, Cherian A, Nordström L, Grubmüller H, de Groot BL, et al. GROMACS in the cloud: a global supercomputer to speed up alchemical drug design. J Chem Inf Model. 2022;62(7):1691-711. https://doi.org/10.1021/acs.jcim.2c00044

48. Teijlingen AHWA, Swanson Lau KHA, Tuttle T. Constant pH coarse-grained molecular dynamics with stochastic charge neutralization. J Phys Chem Lett. 2022;13(18):4046-51. https://doi.org/10.1021/acs.jpclett.2c00544

49. Nettey-Oppong EE, Muhammad R, Ali A, Jeong HW, Seok YS, Kim SW, et al. The impact of temperature and pressure on the structural stability of solvated solid-state conformations of *Bombyx mori* silk fibroins: insights from molecular dynamics simulations. Materials. 2024;17(23):5686. https://doi.org/10.3390/ma17235686

50. Kumari R, Kumar R, Lynn A. g_mmpbsa - a GROMACS tool for high-throughput MM-PBSA calculations. J Chem Inf Model. 2014;54 (7):1951-62. https://doi.org/10.1021/ci500020m

51. Oláh J, Szénási T, Lehotzky A, Norris V, Ovádi J. Challenges in discovering drugs that target the protein-protein interactions of disordered proteins. Int J Mol Sci. 2022;23(3):1550.https://doi.org/10.3390/ijms23031550

52. Borhani DW, Shaw DE. The future of molecular dynamics simulations in drug discovery. J Comput Aided Mol Des. 2012;26 (1):15-26. https://doi.org/10.1007/s10822-011-9517-y

53. Hassan AM, Gattan HS, Faizo AA, Alruhaili MH, Alharbi AS, Bajrai LH, et al. Evaluating the binding potential and stability of drug-like compounds with the monkeypox virus VP39 protein using molecular dynamics simulations and free energy analysis. Pharmaceuticals. 2024;17 (12):1617. https://doi.org/10.3390/ph17121617

54. Li Z, Gu J, Zhuang H, Kang L, Zhao X, Guo Q. Adaptive molecular docking method based on information entropy genetic algorithm. Appl Soft Comput. 2015;26:299-302. https://doi.org/10.1016/j.asoc.2014.10.008

55. Lobanov MY, Bogatyreva NS, Galzitskaya OV. Radius of gyration as an indicator of protein structure compactness. Mol Biol (Mosk). 2008;42(4):623-28. https://doi.org/10.1134/S0026893308040195

56. Ahmed MC, Crehuet R, Lindorff-Larsen K. Computing, analysing and comparing the radius of gyration and hydrodynamic radius in conformational ensembles of intrinsically disordered proteins. Methods Mol Biol. 2020;2141:429-45. https://doi.org/10.1007/978-1-0716-0524-0_21

57. Sawant S, Patil R, Khawate M, Zambre V, Shilimkar V, Jagtap S. Computational assessment of select antiviral phytochemicals as potential SARS-CoV-2 main protease inhibitors: molecular dynamics guided ensemble docking and extended molecular dynamics. In Silico Pharmacol. 2021;9(1):44. https://doi.org/10.1007/s40203-021-00107-9

58. Pradhan R, Dandawate P, Vyas A, Padhye S, Biersack B, Schobert R, et al. From body art to anticancer activities: perspectives on medicinal properties of henna. Curr Drug Targets. 2012;13(14):1777-98. https://doi.org/10.2174/138945012804545588

59. Kumar S, Sharma PP, Upadhyay C, Kempaiah P, Rathi B, Poonam N. Multi-targeting approach for Nsp3, Nsp9, Nsp12 and Nsp15 proteins of SARS-CoV-2 by diosmin as illustrated by molecular docking and molecular dynamics simulation methodologies. Methods. 2021;195:44-56. https://doi.org/10.1016/j.ymeth.2021.02.017

60. Roy A, Khan A, Ahmad I, Alghamdi S, Rajab BS, Babalghith AO, et al. Flavonoids a bioactive compound from medicinal plants and its therapeutic applications. Biomed Res Int. 2022;2022:5445291. https://doi.org/10.1155/2022/5445291

61. Lozza L, Moura-Alves P, Domaszewska T, Lage Crespo C, Streata I, Kreuchwig A, et al. The henna pigment *Lawsonia inermis* (L.) pigment Lawsone activates the aryl hydrocarbon receptor and impacts skin homeostasis. Sci Rep. 2019;9(1):10878. https://doi.org/10.1038/s41598-019-47350-x

62. Xiang S, Li Y, Khan SN, Zhang W, Yuan G, Cui J. Exploiting the anticancer, antimicrobial and antiviral potential of naphthoquinone derivatives: recent advances and future prospects. Pharmaceuticals. 2025;18(3):350. https://doi.org/10.3390/ph18030350

63. Widhalm JR, Rhodes D. Biosynthesis and molecular actions of specialized 1,4-naphthoquinone natural products produced by horticultural plants. Hortic Res. 2016;3:16046. https://doi.org/10.1038/hortres.2016.46

64. Yadav S, Sharma A, Nayik GA, Cooper R, Bhardwaj G, Sohal HS, et al. Review of shikonin and derivatives: isolation, chemistry, biosynthesis, pharmacology and toxicology. Front Pharmacol. 2022;13:905755. https://doi.org/10.3389/fphar.2022.905755

65. Giongo V, Falanga A, De Melo CPP, da Silva GB, Bellavita R, De-Simone SG, et al. Antiviral potential of naphthoquinone derivatives encapsulated within liposomes. Molecules. 2021;26(21):6440. https://doi.org/10.3390/molecules26216440

66. Tandon VK, Yadav DB, Singh RV, Vaish M, Chaturvedi AK, Shukla PK. Synthesis and biological evaluation of novel 1,4-naphthoquinone derivatives as antibacterial and antiviral agents. Bioorg Med Chem Lett. 2005;15(14):3463-6. https://doi.org/10.1016/j.bmcl.2005.04.075

67. Moraes VT, Caires FJ, Da Silva-Neto PV, Mendonça JN, Fraga-Silva TFC, Fontanezi BB, et al. Naphthoquinone derivatives as potential immunomodulators: prospective for COVID-19 treatment. RSC Adv. 2024;14(10):6532-41. https://doi.org/10.1039/D3RA08173G

68. Vasić V, Momić T, Petković M, Krstić D. $Na^+$, $K^+$-ATPase as the target enzyme for organic and inorganic compounds. Sensors. 2008;8(12):8321-60. https://doi.org/10.3390/s8128321

69. De Souza E Souza KF, Rabelo VWH, Abreu PA, Santos CCC, Abreu Do Amaral E Silva N, De Luna D, et al. Synthetic naphthoquinone inhibits herpes simplex virus type-1 replication targeting $Na^+$, $K^+$ ATPase. ACS Omega. 2024;9(34):36835-46. https://doi.org/10.1021/acsomega.4c05904

70. Verma S, Newar J, Manoswini M, Dhal AK, Ghatak A. Interactions of the Nsp3 proteins of CHIKV with the human host protein NAP1 plays a significant role in viral pathogenesis - an in silico study. Hum Genet. 2023;36:201182. https://doi.org/10.1016/j.humgen.2023.201182

71. Tuan NA, Khanh PN, Ha NX, Binh TC, Khanh ND, Oanh TT. Compounds isolated from *Lawsonia inermis* L. collected in Vietnam and evaluation of their potential activity against the main protease of SARS-CoV-2 using in silico molecular docking and molecular dynamic simulation. Nat Prod Commun. 2022;17(10):1-14. https://doi.org/10.1177/1934578X221125161

72. Halder SK, Sultana I, Shuvo MN, Shil A, Himel MK, Hasan MA, et al. In silico identification and analysis of potentially bioactive antiviral phytochemicals against SARS-CoV-2: a molecular docking and dynamics simulation approach. Biomed Res Int. 2023;2023:5469258. https://doi.org/10.1155/2023/5469258

73. Ilyas M, Muhammad S, Iqbal J, Amin S, Al-Sehemi AG, Algarni H, et al. In-sighting isatin derivatives as potential antiviral agents against NSP3 of COVID-19. Chem Pap. 2022;76(10):6271-85. https://doi.org/10.1007/s11696-022-02298-7

74. Joshi R, Gaikwad H, Soge B, Alshammari A, Albekairi NA, Kabra A, et al. Exploring pyrazolines as potential inhibitors of NSP3-macrodomain of SARS-CoV-2: synthesis and in silico analysis. Sci Rep. 2025;15(1). https://doi.org/10.1038/s41598-024-81711-5

75. Roshni J, Vaishali R, Ganesh KS, Dharani N, Alzahrani KJ, Banjer HJ, et al. Multi-target potential of Indian phytochemicals against SARS-CoV-2: a docking, molecular dynamics and MM-GBSA approach extended to Omicron B.1.1.529. J Infect Public Health. 2022;15(6):662-9. https://doi.org/10.1016/j.jiph.2022.05.002


## Additional information


**Peer review**: Publisher thanks Sectional Editor and the other anonymous reviewers for their contribution to the peer review of this work.

**Reprints & permissions information** is available at https://horizonepublishing.com/journals/index.php/PST/open_access_policy

**Publisher's Note**: Horizon e-Publishing Group remains neutral with regard to jurisdictional claims in published maps and institutional affiliations.

**Indexing**: Plant Science Today, published by Horizon e-Publishing Group, is covered by Scopus, Web of Science, BIOSIS Previews, Clarivate Analytics, NAAS, UGC Care, etcSee https://horizonepublishing.com/journals/index.php/PST/indexing_abstracting





**Publisher information:** Plant Science Today is published by HORIZON e-Publishing Group with support from Empirion Publishers Private Limited, Thiruvananthapuram, India.